Mapana - Journal of Sciences
2023, Vol. 22, Special Issue 2, 297-318
ISSN 0975-3303 | https://doi.org/10.12723/mjs.sp2.17

Comparative Study for Image Fusion Using Various Deep Learning Algorithms

Anna Saro Vijendran* & Kalaivani Ramasamy*

Abstract

Image fusions are that join medical images from many modalities like CTS (Computed Tomography Scans) and MRI (Magnetic Resonance Imaging) with the aim of presenting better clinical content to clinicians and doctorsfor planning treatments or therapies. Prior studies based on white images have showed issues in early predictions of brain tumours like inaccurate image. This study attempts to overcome this issue by comparing MUNets (Modified-UNets), MCNNs (Multi-Cascaded ConvolutionNeural Networks) with fully connected CRFs (Conditional Random Fields), MFCLs (Modified Fully Connected Layers), TA-cGANs (Tissue-Aware conditional Generative Adversarial Networks) and EL (Ensemble Learning) algorithms. Furthermore, in order to enhance image quality and enable the early diagnosis of brain tumours, novel multimodal medical image fusion techniques are being examined. Furthermore, it is suggested that the EL algorithm improve MRI brain image fusion performance. The four primary phases of the suggested system are segmentation, image synthesis, feature extraction, and noise reduction. To eliminate noises, AMFs (Adaptive Median Filters) are used for reducing noises in MRI images and thus assist in enhancing classification accuracies. These features are taken into segmentation process using RGKMC (Region Growing based K-Means Clustering). Feature extractions are performed using AFFOCNNs (Adaptive FireFly Optimization based Convolution Neural Networks) algorithm which computes necessary and prominent

* Department of Computer Application, Sri Ramakrishna College of Arts & Science, Coimbatore – 641044, Tamil Nadu, India; E-mail: saroviji@rediffmail.com, tokalai2011@gmail.com

features. Subsequently, MCCNNs, MUNets, MFCLs, TA-cGANs and EL algorithms are applied for classifications through training and testing models. They classify features more accurately using their informative features. The experimental result proves that ELalgorithms provides better classificationsthan the MCCNNs, MUNets, MFCLs and TA-cGANs when evaluated in terms of higher accuracies, precisions, recalls and reduced MSEs (Mean Square Errors), execution times

Keywords: Image fusion,Modified-UNet (MUNet), Multi-Cascaded Convolutional Neural Network (MCCNN) with fully connected Conditional Random Fields (CRFs), Modified Fully Connected Layer (MFCL), Tissue-Aware conditional Generative Adversarial Network (TA-cGAN) and Ensemble Learning (EL)

1. Introduction

Medical image fusion combines many images taken with various modalities to improve image quality while maintaining distinct image features. Combining techniques enhances the visualisation and clarity of information, assisting medical professionals in diagnosing and assessing illness conditions. High-tech medical imaging technology is an essential component of many applications, including diagnostics, research, and treatment [1]. Medical image fusion refers to the concept of integrating images from multiple imaging methods, such as CTS, MRI, PET (computed emission tomography) and SPECT (computed tomography). Single image emissivity), in order to increase the content of the image. While MRI imaging provides superior information on soft tissues that are denser and more deformed, CTS imaging provides the best data for medical diagnosis on denser tissues with less deformation than [2].

A dimensionality reduction method used in image synthesis is called feature extraction. They increase accuracy while decreasing computing complexity. Apart from feature selection, one effective way to lower the dimensionality of data is by feature extraction. More specifically, the hyperspectral images are first subjected to linear transformations and then projected onto various feature spaces. Then, only the crucial elements are included in the categorization process [3]. Numerous techniques for reducing dimensionality have been employed, encompassing both supervised

approaches like linear discriminant analysis (LDA) and unsupervised techniques like principal component analysis (PCA) and independent component analysis (ICA). PCA-based methods can guarantee that a limited number of crucial PCs (primary components) are needed to preserve a majority of hyperspectral image information.

This research work's primary goal is effective image synthesis from MRI scans. Though many methods and research have been created, image quality has not improved significantly. Traditional techniques take a long time and yield inaccurate imaging findings and for enhancing overall performances of systems while addressing the aforementioned issues, this study presents MUNets, MFCL, TA-cGAN, and EL approaches. Image fusion, segmentation, noise reduction and feature extraction are the main contributions to this research work. The technique proposed in this study uses excellent algorithms to produce more accurate results in the provided collection of MRI images.

This work's remaining sections are organised as follows: Section 2 discusses an overview of the literature on brain tumour image segmentation and fusion. Section 3 presents a thorough technique for image fusion utilising MRI scans. Section 4 presents the outcomes of the experiment. Section 5 marks the end of the document.

2. Related Work

Multimodal medical image fusions based on VMDs (Variational Mode Decompositions) and LEM (Local Energy Maxima) was introduced by Polinati et al in [4]. In order to efficiently extract edge information while minimising boundary distortions, the study decomposed source images into numerous IMFs (intrinsic mode functions) with the aid of VMDs and for combining IMFs based on local information, LEM was applied. By carefully conserving the necessary spatial information, LEM plays significant parts in the quality of fused images where the strategy's effectiveness was assessed using subjective/objective metrics. Comparing the technique to other existing and well-regarded fusion approaches, the experimental study reveals that it yields promising outcomes.

In [5], Liu et al (2017) proposed using deep CNNs (Convolution Neural Networks) to encode the mapping. Qualitative image

patches with their corresponding blurred versions are trained by CNNs. This theory's primary innovation is in its ability to create activity level measurements and synthesis rules simultaneously using CNN learning, a capability that resolves a problem with earlier synthesis techniques. The novel multifocal image fusion technology is primarily applied in this work. According to experimental findings, this method can provide the most sophisticated artificial performance in terms of objective evaluation and image quality. The parallel computing approach has a fast enough computation speed for daily use. Experiments also briefly demonstrated CNN's potential for additional image synthesis issues.

Yan et al. (2020) pointed out in [6] that multi-view approaches preserve variety of data properties. Hence, in order to advance hash learning, the study presented multi-view deep neural networks and created a retrieval model that was effective, creative, and significantly improved retrieval performances. Their supervised multi-view hash model improved multi-view information using neural networks. Their brand-new hash learning technique combined deep learning with multi-view learning. By employing efficient techniques to assess view stability, this method has actively investigated the interaction between views, impacting the path of network optimisation. It is necessary to build a variety of multi-data fusion approaches and keep the benefits of convolution and many views in order to maintain the Hamming space.

Tan et al. (2021) proposed MLEPF (Multi-Level Edge Preservation Filter)-based deconstructed multi-modal medical image fusion method in [7]. First, using weighed mean curvature filtering, MLEPF models divide multimodal medical images into three types of layers namely fine and coarse structures, and base layers. Secondly, fine and coarse structure layers are concatenated using PCNN (pulse coupled neural network) gradient domain synthesis technique, while the base layers are concatenated using different characteristic features. Rise. The combined image is then created by blending three separate merged layer types. Six separate disease datasets and one normal dataset containing more than 100 image pairs were used in the experiments.

3. Methodology

To increase the effectiveness of image synthesis, the MCCNN, MUNets, MFCL, TA-cGAN, and EL techniques are compared and assessed in this study.

3.1 Input Image Datasets

BraTS 2018 is a dataset that provides multimodality 3D brain MRIs and brain cancer classifications assessed by specialists, using four MRI modalities for each case: T1, T1c, T2 and FLAIR. Three tumour subregions were found: necrotic and non-enhancing tumour core, peritumoural edema, and tumour growth. Three nested subregions—the whole tumour, the centre tumour, and the expanding tumour—were used to compile the observations. The data is based on several MRI scanners at 19 different universities.

3.2 Denoising Using AMFs

In this study, the AMF algorithm is used for denoising, with the goal of eliminating unnecessary noise from specific image graphs. Its primary purpose is to offer a dependable and efficient model to enhance imaging outcomes when there is a lot of noise present. AMF uses spatial processing to identify which image pixels are impacted by noise [8]. AMF recognises pixels as noise by comparing each pixel in the image with its neighbours. Both the comparison criterion and the neighbourhood's size are scalable [9]. Adaptive filter windows expand to accommodate amounts of noises expected in specific areas. Noisy pixels in regions are used to calculate window sizes in regions (1). To obtain best MSE-based results, exhaustive simulations are used to establish window resizing thresholds based on amounts of noisy pixels in areas.

$$W(M) = \sum_{P} C(p, D_p) + \sum_{q \in N_p} T\left[\left|M_P - M_q\right| = 1\right] + \sum_{q \in N_p} T\left[\left|M_P - M_q\right| > 1\right]$$

W stands for window matching function, while M stands for the optimal solution of W.In the given image, the actual pixel is p, and q is a neighbor pixel of p. N_P represents the set of pixels next to p. M_P and M_q are the corresponding estimation windows of p and q, respectively. C represents costs of given corresponding windows T[.] implies logical functions that evaluate statements and returns 1 if they are true and 0 if they are false. Expanded window sizes

according to equation (1) when there are no noise-free pixels in windows or medians of windows are noisy pixels.

3.3 Brain Tumour Segmentations Using RGKMC Algorithm

The RGKMC algorithm efficiently performs brain tumour segmentation in this work. The technique of distinguishing a brain tumour from healthy brain tissue is known as brain tumour segmentation; in standard clinical practise, this information is helpful for diagnosis and therapy planning. This is still a challenging procedure, nevertheless, because of the tumours' asymmetrical form and hazy borders. In this study, an algorithm called RGKMC is suggested to solve the previously described problem. Based on the cluster's initial centroid, KMC is a helpful clustering technique for classifying similar data [10]. The centroids of the clusters are found using the concept of Euclidean distance. The images were cut black and white by RGKMC. Because the melanoma in this study was seen in both scans, it could serve as an early sign of a brain tumor. This technique starts with random partitions and (ii) reallocates data items to clusters with closest centers to continuously calculate the current cluster center or mean vector of each cluster in the data space. It ends when there are no more transfers. This reduces the within-cluster variance, which is the sum of the squares of the variations between the data attributes and their local corresponding cluster centroids.

3.4 Feature Extraction Using AFFOCNNs

The AFFOCNN algorithm is used in this study to extract more informative features by selecting the most pertinent values for feature extraction. The feature extraction step uses three convolutional layers to extract properties from the raw image. Finding characteristics or attributes is a more crucial stage in image fusion methods.

The best method is employed in CNN, which uses convolution kernel training and efficient initialization. Consequently, using Google's convolutional layer is advised. This is well-equipped on ImageNet as the primary CONV1 (Convolutional Layer) makes use of the image's effective qualities using 64 convolutional kernels, each measuring 7 by 7. Even though CONV1 calls for a wider range of

identification, more examples might be employed. It is evident that not every aspect of a image must be shown throughout the merging process. The second and third convolutional layers that are added to filter the properties acquired by CONV1 are called CONV2 and CONV3 and ultimately provide a combinable attribute graph. A portion of the image data can be absent if the input image is not sampled correctly. This missing data will have an impact on the outcomes during the feature extraction phase. For the core of every convolutional layer, update the tempo and padding parameters in a consistent manner.

This work examines the use of AFFO in parameter updating and ongoing exploration of the best deep learning configuration to provide efficient outcomes. The primary objective is to use the AFFO technique to discover the best aspects after choosing highly appropriate components to produce a presentation worthy of CNN.

Real firefly' social and physiological traits have an impact on the FA (Firefly Algorithm) [11]. Genuine fireflies produce brief, regular bursts of light that serve as a warning of impending danger as well as an aid in relationship attraction and communication. FA creates this flickering behaviour by utilising the problem's objective function for optimisation. FA operates on the same premise as firefly flashing lights. The brightness of the light encourages a firefly group to go to appealing and intense spots that are planned to create the best resolution over the sought-after location.

A number of the firefly traits are normalised by these methods and demonstrated below [12]:

(i) Fireflies are drawn to a wide range of people, regardless of sex.

(ii) If there are two fireflies, the brighter of the two will attract the dimmer one as a firefly's appeal is directly correlated with how brilliant it is. The firefly will randomly shift course if it is unable to detect the neighbouring brighter firefly.

This study presents a novel fitness function that is provided by and assumes the running duration and accuracy as.

$$f(x) = \frac{\left(\frac{I_d}{I_t}\right) \times \left(\frac{I_p}{p_{init}i}\right)}{exp^{-e_E/e_M + H_{accuracy}}}$$

where I_d represents dropped image feature counts. m_t represents counts of features sent with high accuracy

I_p represents pixels in images i

$P_{init}{}^{i}$ represents initial images

e_E represents execution times and e_M represents maximum allowable delays

$$x_i = x_i + \beta_o e^{-\gamma r^2}\left(x_j - x_i\right) + \propto (rand - \frac{1}{2}) \quad (3)$$

Where x_i and x_j represents distanced between firefly's features

Every feature's fitness value is computed within the population. In first generations, fireflies' suitable values are determined and pixel counts in batches are randomly allocated. The two fireflies to be chosen were then chosen through a selection procedure. The firefly was chosen for the following generation because of its increased brightness and maximum fitness score.

3.5 Image Fusion Using Deep Learning Algorithms

3.5.1 MUNets

The suggested approach employs a residual method to filter replication of attribute plot data with poor resolution. However, unlike current approaches, projected network maintains the residual path after assembly.

This technique may be adjusted to blend with additional convolutional layers in the skip connections and confine high-resolution edge data from attribute cells flowing via the skip connections. Permeation data were collected in order to assess this adaptive filter's effectiveness. Data on penetration must be PD.

$$PD = \begin{Bmatrix} -0.5, \text{ if } \mathrm{FMy(p,q)} < 0.01 \\ \sum \frac{\mathrm{FMx(p,q)}}{\mathrm{FMy(p,q)}}, \mathrm{p,q} \in \text{object tag(p,q)}, \text{Otherwise} \end{Bmatrix} \quad (4)$$

Where,

FMx-standardized attribute visualisation behind the residual path in the skip connection

Plot of FMy-standardized attributes before residual track

The range of any standardised attribute plot is [0, 1].

When $FMy(p, q) < 0.01$ the permeation rate can be set to -0.5, indicating that the skip link has no noteworthy characteristics.

Some of the tested changes were applied to the updated UNets. Initially, each block of the encoder made use of the residual connection. There were 3 convolution layers for each encoder block. The new encoder block's input was added to the result that the preceding encoder block had produced. The max pooling layer was updated using the final convolution layer's stride of 2, which was 2. UNets model was used as the foundation for the stack idea. In the instance of modified UNets, dual UNets were taken into consideration rather than a single UNets, with UNet's output being routed back to its input. Utilising this repeating design pattern uses the fewest possible parameters and conserves GPU RAM. In the initial iteration and each subsequent iteration, the cost function was loaded with costs from the UNet. The training can be effectively accelerated by including the intermediate outcome in the cost estimation process.

3.5.2 MCCNNs

MCCNNs merge many networks to create a multi-cascaded network architectures as seen in Fig. 1. The segmentation of brain gliomas using the Input Cascade CNN architectures [13] attained state-of-the-art performance. Two cascading forms have been applied to accentuate and enlarge this building. Articulations are acts of cascading shapes into an array below the input and treating the array above the output as additional visual channels to control the formation of the second array. Additionally, multi-layer CNN designs can be unified by feeding the feature map generated by simple classification into a network of layers before passing it to the final classification layer.. Since the neurons in the soft-max output layer are directly cascaded with the previous output, training the network is more likely to assume that to produce smoother edges,

the center pixel label must be equivalent with the surrounding environment. Two multilayer network architectures are examined in this study, referred to as MCCNN1 and MCCNN2, respectively.

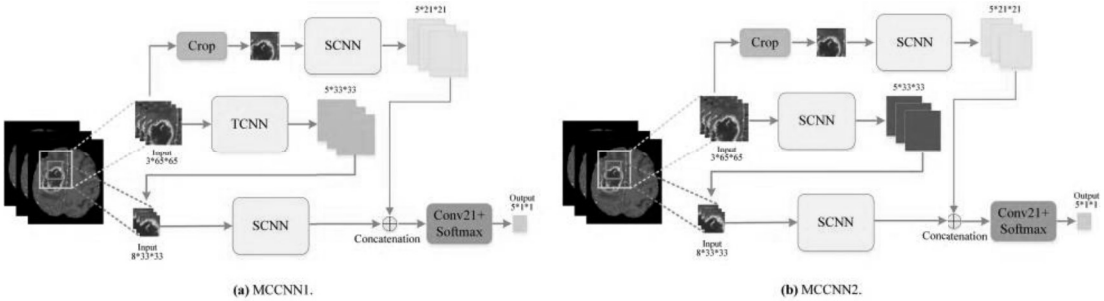

Fig 1MCCNN1 and MCCNN2 architecture

The TSCNN architecture is used by MCCNN1 as a straightforward concatenation, as seen in Fig. 1(a). In this architecture, we extract features from image patches using a two-path network and utilise singular paths deep networks to learn features from smaller image patches. In order to facilitate the extraction of contextual information and other local aspects, an additional single route network is incorporated to ascertain details about the tumor's edges.

Larger image patches are cropped in MCCNN2 using the SSCNN architecture, as shown in Fig. 1(b), and then use the smaller image patches as input to additional one-path networks to determine local image features, such as brain tumor edge information. The previous final result layers connect the obtained intermediate results. The size of the growing plots can be adjusted to meet specific requirements. By combining multiple cascading shapes and integrating information at multiple scales, it is possible to not only account for label dependence but also increase glioma segmentation performances.

3.5.3 MFCLs

Regular multilayer Perceptron is the layer that is completely linked. Consideration is given to a classifier in the output layer. Typically, the classifier is the Softmax activation function. When a network is fully linked, all of the neurons in one layer are related to all of the neurons in the layer above. to use the characteristics of the output

from the preceding layer to categorise the input image based on the training data.

The goal of image fusion is to keep complementary parts of the separate source images while reducing extraneous information and distortion. Performance measures are thus critical for comparing the outputs of various algorithms and determining the effectiveness of the synthesis [8]. To appropriately diagnose and treat brain cancer, the type, size, location, and spread of the tumour must all be identified. The use of fused MRI brain imaging speeds up the identification and diagnosis of brain cancer. They produce better results than an MRI alone. Telemedicine and its applications are revolutionising medical services in some cases, thanks to new techniques for remote diagnosis and faster first aid supply [14]. In reality, the term "feature extraction" refers to strategies for combining variables to overcome these challenges and adequately characterise the data.

The majority of computer science students believe that well-optimized feature extraction—which may be gathered from several visual levels—is the true key to effective model creation.

- Low-level content: This type of material consists of visual image elements including colour, texture, and form.
- Level 2-intermediate content: It deals with the existence or configuration of various kinds of items, settings, and scenarios.
- High-level content: This content consists of feelings, perceptions, and interpretations connected to the blending of cognitive elements.

The training sample is introduced in the input layer of this suggested system, which employs the CNN algorithm technique during the training phase. Subsequently, the outputs of the artificial images undergo evaluation and comparison with the output, input, output matrices, and hidden layer predictions. The input image is split into pixels in the first stage of this procedure. In two-dimensional visuals, these pixels are seen as arrays of two dimensions. Certainly, every pixel has a value (ranging from 0 to 255). White is represented by the number 255 and black by the number 0. Grey scale is one of these measurements. Based on this knowledge, the system will also begin processing data. This is a three-dimensional array containing layers

for colour images in blue, green, and red. These colours have values between 0 and 255. The values of the three layers can be concatenated to form a colour. PSNR computes the error and transmission time in this phase. Model performance is optimised with the aid of updated feature weights and metrics. The output layer has an image synthesis display and is operated by a button. The brain's MRI scans are considered and evaluated from many angles. To create a clear image, images from various viewpoints are combined and taken into consideration. The image is stitched based on the features.

3.5.4. TA-cGANs

TA-cGAN. Conversely comprises of two more subnetworks, the discriminator and generator and intended for image-to-image translation, meaning that it takes in several images (IM, which is the MRI image, and its associated label map IL), merges them, and produces the IF image. As opposed to this, image-to-image translation was the primary use of the original GAN. Further details on the TA-cGAN network architecture are given in the ensuing section.

Generator

The generators are built using a U-Nets-based technique that combines high-level features from deep decoding layers with low-level features from shallow encoding layers via jumper access connections. Furthermore, the skip connection method can be used to alleviate the problem of gradient fading. U-Net has been shown to be beneficial for a variety of imaging applications, including image synthesis, using the concept of skipped connections [15].. The encoder consists of six down-sampled layers that generate convolutions using batch normalization and rectified linear unit activations, as well as 33 loads with two steps in each direction. Notably, we avoid using pooling operations since they would limit feature maps' spatial resolution and prevent the network from capturing tiny features in MRI images. Additionally, each down-sample layer uses zero padding with 11. Decoder portions consist of six up-sample layers and last layers do convolution operations using 11 filters while the first five layers execute convolution-batch normalizations- rectified linear unit operations.

Discriminator

Unlike generators G, the main goals of discriminators D are to solve classification problems. In this work, the main goals of discriminators D are to distinguish pairs of merged images (IF merged image and IL label map) from the pair of MRI images (IM MRI image and IL label map) [16] [17].

3.5.5 Ensemble Learning (EL) Algorithm

In this section, TA-cGANs algorithm combines GANs and ANNs (Artificial Neural Networks) for its Ensemble Learning (EL) to improve multi view image fusion performances. GANs are fine-tuned using ANNs. General architecture of the generator and discriminator is briefly illustrated in Fig 2 and 3.

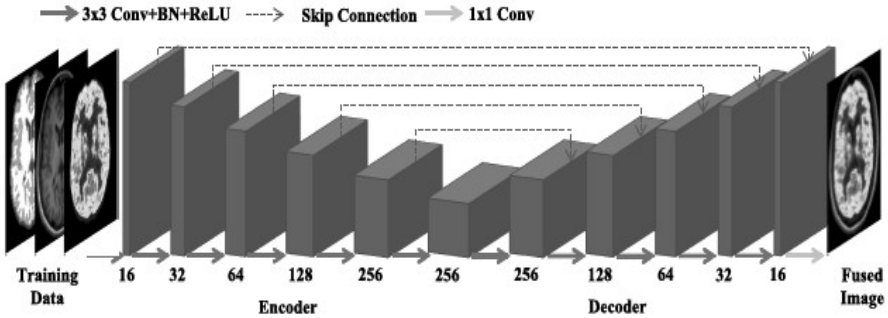

Fig 2 Network architecture of the Generator

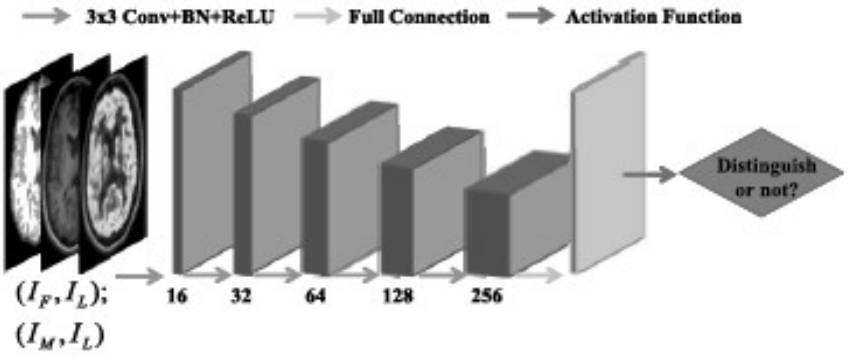

Fig 3 Network architecture of the discriminator

Discriminators D are straightforward CNNs with sigmoid activations and one fully connected layer, and five convolutional layers. The aforementioned convolutional layers, which mimic the

coding structure of the G generator, carry out the convolution-BN-ReLU procedures.

One notable use of conditional generative adversarial networks is the integration of MRI and PET images. MRI's distinguishing features include high spatial resolution, distinct structural information about soft tissues, and colour information that represents the functioning characteristics of the tissue. Healthcare practitioners are employing TA-cGAN-based brain MRI image fusion techniques to assist in more precise diagnosis of the condition.

ANNs are used to learn and accumulate knowledge. The input, hidden, and output layers of an ANN are divided into three phases. Input layers gather input images, which are then processed to provide a "n" number of inputs. These procedures follow a set of weights. Weights assist neural networks solve issues by providing information [26]. After some beneficial hidden extraction, the hidden information is taken from the input layer and sent to the output layer. In this case, ANNs are utilised to find high-quality image characteristics. Using ANNs, the MRI image dataset is trained, and state characteristics are categorised during testing.

Training of the Discriminators

Generators generate $2n$ batches $\{B_{a1}, \ldots, B_{an}, B_{g1}, \ldots, B_{gn}\}$ of b pixels for T epochs and fixed $\boldsymbol{\varphi}$ i.e. The actual data sets are not used to calculate quality scores. Furthermore, the discriminator of each dataset i takes a sample of Briof b points from the dataset Di that is accessible. Each created batch is sent by the generator to Baito for each tuple, from which the loss value is computed as follows:

$$L_i(\theta_i) = \frac{1}{b}\left[\sum_{x \epsilon B_{r_i}} log D_{\theta_i}(x) + \sum_{x \epsilon B \alpha_i} \log\left(1 - D_{\theta_i}(x)\right)\right] \qquad (5)$$

$L_i(\theta_i)$ characterizes value approximations of functions for datasets' discriminators in (1) and by using gradient descents like Adam optimizers [27], datasets are updated with their own weights θ_i

Training of the Central Generator

Every T epochs, every database i uses B_{gi} to calculate the following loss:

$$L_i^g = \frac{1}{b}\left[\sum_{x \epsilon B_{g_i}} \log\left(1 - D_{\theta_i}(x)\right)\right] \qquad (6)$$

Which implies approximations of value functions for database generators in (6).

TA-cGANs utilises joint losses including spectral loss *Lspec* urges fused images to contain similar colour information (Characterized by the pixel intensities of MRI images; The structural losses L_{Str} attempts to make fused images have similar structure information (Characterized by MRI image gradients) as those of MRI images; The adversarial losses L_{Adv} aims to add more detailed information to fused images; $\lambda_1, \lambda_2 \; and \; \lambda_3$ are corresponding weights for spectral loss, structural loss and adversarial loss, respectively. Fig 4 shows the overall block diagram of the comparative study

4. Experimental Result

The BraTS 2018 dataset offers multi-modality 3D brain MRI scans and brain cancer analysis recognised by healthcare experts (T1, T1c, T2, and FLAIR), with four separate MRI modalities per patient. The three tumour subregions that were noted in the observations were growing tumour, peritumoral edoema, necrotic tumour core, and absence of enhancement. The BraTS 2018 dataset offers multi-modality 3D brain MRI scans and brain cancer analysis recognised by healthcare experts (T1, T1c, T2, and FLAIR), with four separate MRI modalities per patient. The three tumour subregions that were noted in the observations were growing tumour, peritumoral edoema, necrotic tumour core, and absence of enhancement.

Performance metrics such as accuracies, MSEs, precisions, recalls, F-measures and execution times are considered in evaluations of the proposed technique and comparisons with existing MCCNNs [18], MUNets, MFCLs, TA-cGANs and EL algorithms.

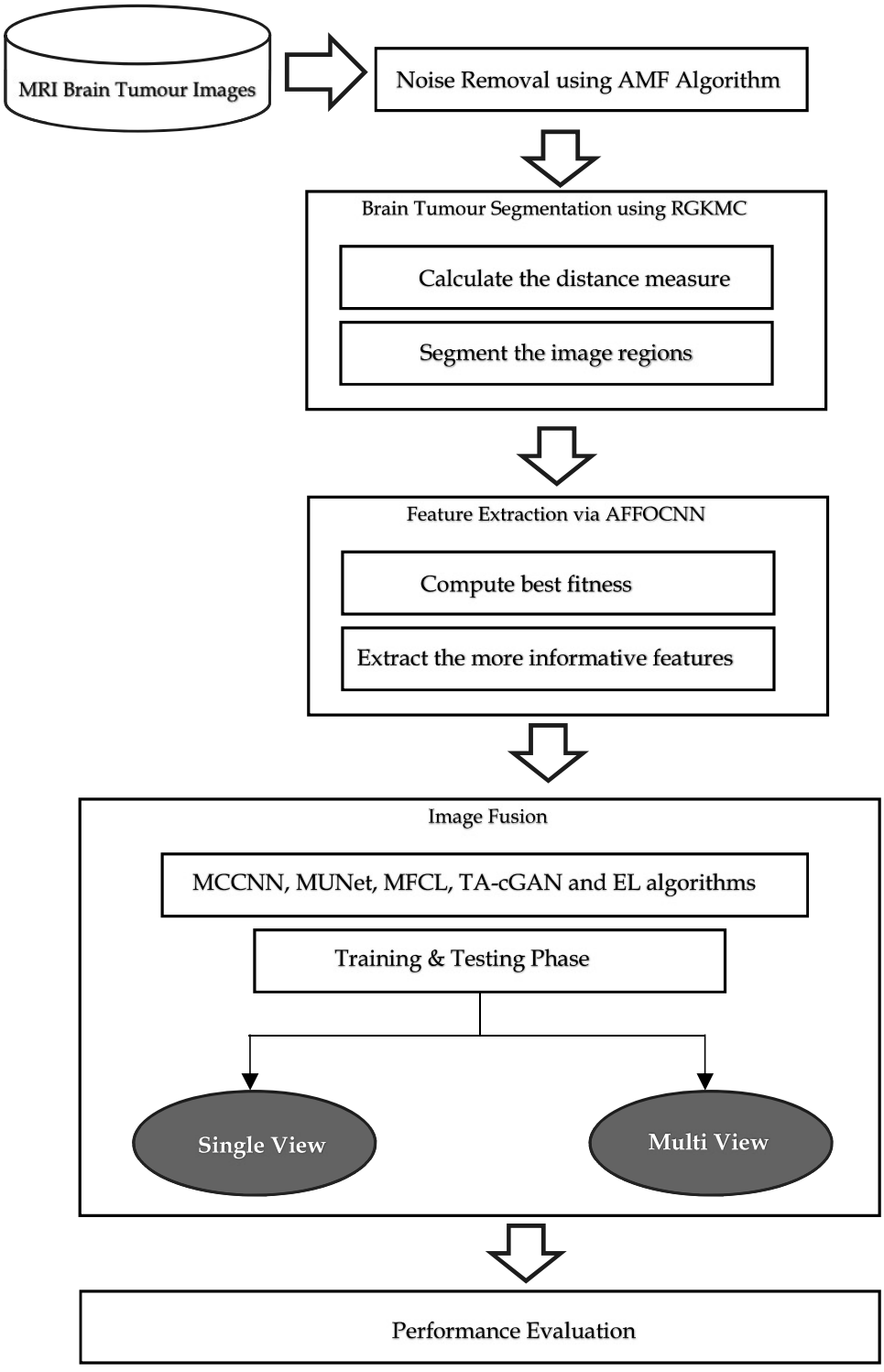

Fig 4 The Overall Block Diagram of the Comparative Study

Accuracy

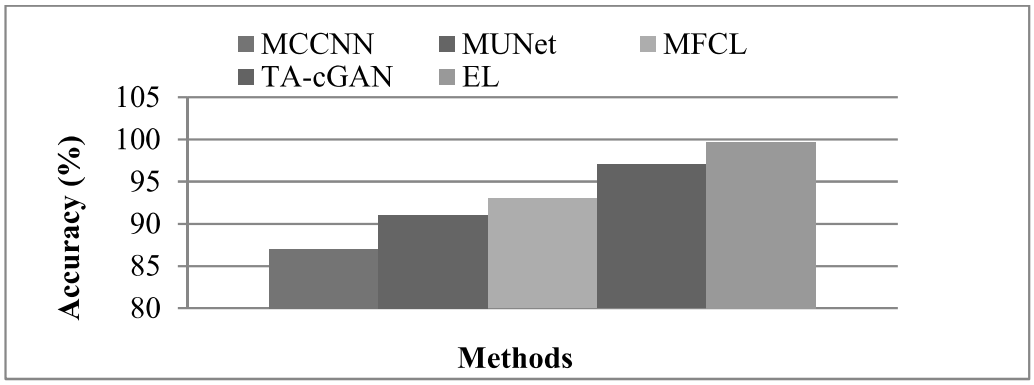

Fig 5 Accuracy

As shown in Fig. 5, the accuracy of the comparison measure is evaluated using the current and proposed methods. The x-axis applies the approaches, while the y-axis shows the exact value. Current approaches such as MFCL, EL, TA-cGAN, MUNets, and MCCNN produce varying levels of accuracy for the presented MRI datasets. By using neighbouring pixels, the proposed area evolution-based segmentation method improves image quality. The effectiveness of image synthesis is increased by AFFOCNN by extracting more useful features. As a result, it was demonstrated that the recommended EL algorithm improved overall performance.

Precision

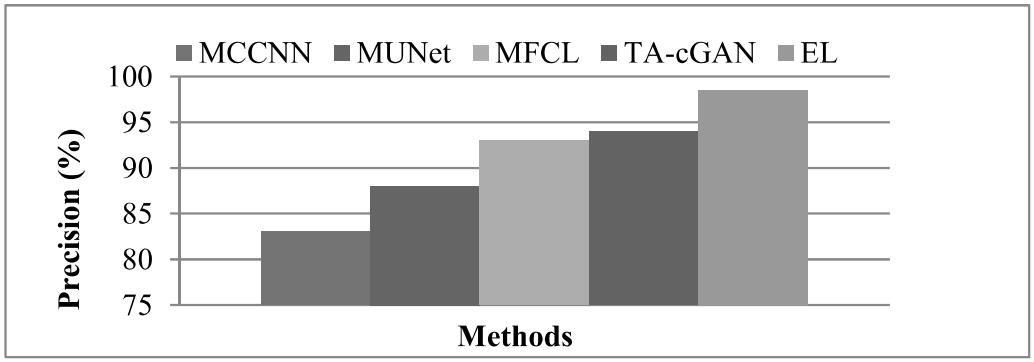

Fig 6 Precision

The precision of the comparison estimation was evaluated using currently used methodologies, as shown in Figure 6. The precise esteem is displayed on the y-axis, while the associated tactics are displayed on the x-axis. The suggested EL technique outperforms the current MCCNN, MUNets, MFCL, and TA-cGAN algorithms in

terms of accuracy. It appears that the proposed EL technique advances the image attributes appropriately for the image amalgamation handle. ANN using TA-cGAN technique aims to improve multi-view image synthesis performance.

Recall

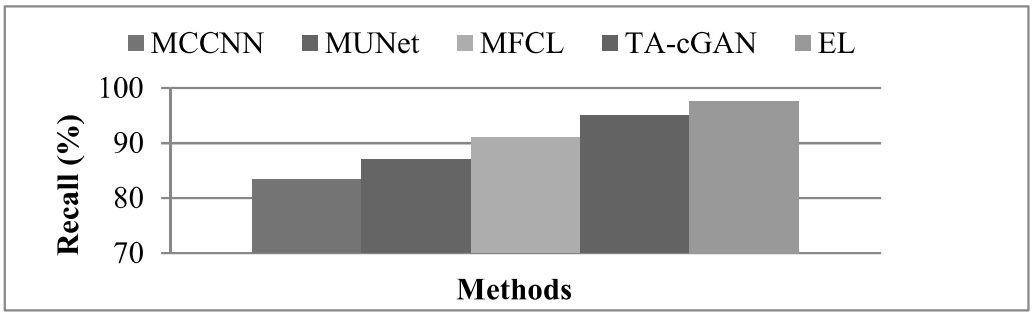

Fig 7 Recall

The recall of the comparison metric is tested using current methodologies, as illustrated in Figure 7. The recall values are displayed on the y-axis, while the methods are displayed on the x-axis. The suggested EL technique outperforms existing methods MCCNN, MUNets, MFCL, and TA-cGAN in terms of recall. The RGKMC and AFFOCNN algorithms, respectively, prioritise the best-correlated pixels and informative features in order to improve image quality. The findings show that the suggested EL approach enhances image characteristics for image synthesis effectively.

F-measure

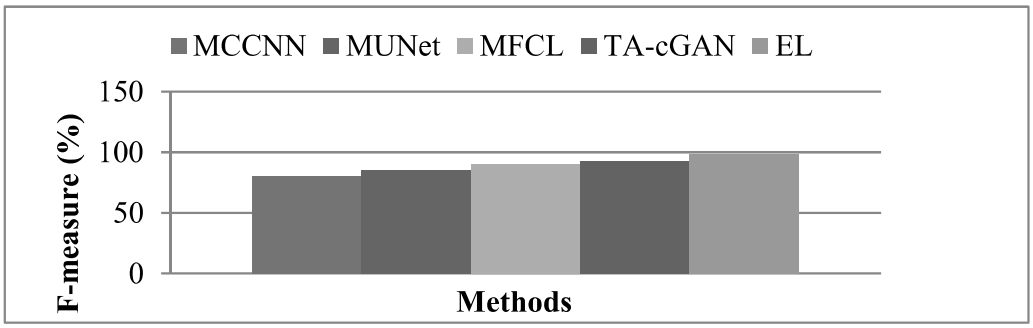

Fig 8 F-measure

Based on Fig. 8, the comparative values of the F-measure utilising the suggested algorithm and the current approach are assessed. The

suggested EL Classifier metric demonstrates an F1 score with 98% prediction power without any mistaken features, while the current techniques, MCCNN, MUNets, MFCL, and TA-cGAN, provide lower F-measures for the given MRI dataset. Therefore, multi-view image fusion for MRI datasets performs better thanks to the suggested complete deep learning approach.

MSE

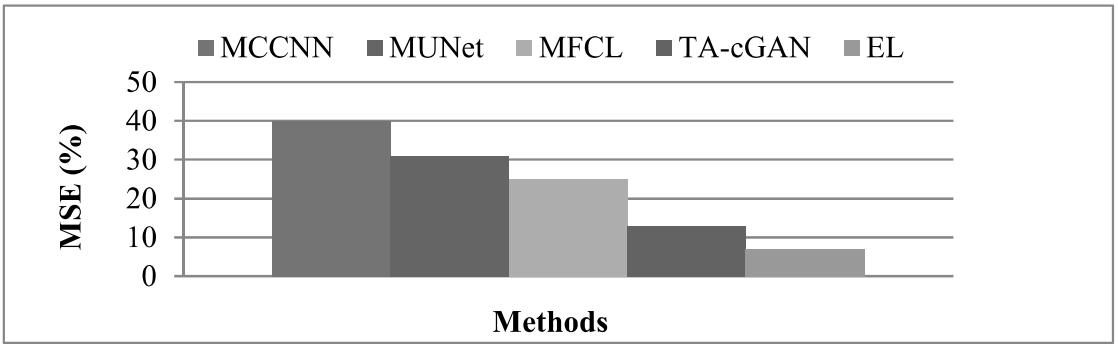

Fig 9 MSE

Figure 9 clearly shows that the comparative degree is measured using the most modern methodologies in MSE. The y-axis displays MSE values, while the x-axis displays strategies. The suggested EL approach outperforms conventional MCCNN, MUNets, MFCL, and TA-cGAN algorithms in terms of MSE. The results reveal that the proposed EL approach significantly advances the execution of multi-view image combining.

Execution Time

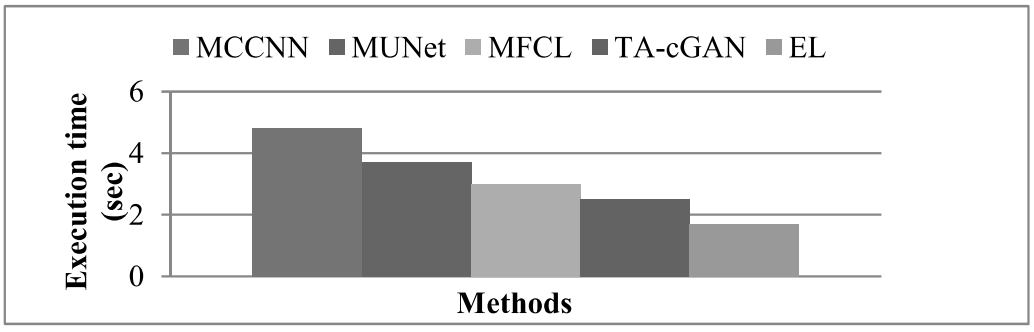

Fig 10 Execution Time

Figure 10 depicts the comparison measurements in terms of execution time using both the proposed and current methodologies. The y-axis displays execution time values, while the x pivot displays the tactics employed. Existing techniques with higher time complexity include MCCNN, MUNet, MFCL, and TA-cGAN, however the suggested EL approach has a reduced time complexity. Based on the data, it is possible to infer that the proposed EL approach is effective.

5. Conclusion

MCCNNs, MUNets, MFCLs, TA-cGANs, and EL algorithms are introduced in this study effort to compare the outcomes of the classification accuracy for the supplied MRI image database significantly. The AMF method is used in this study to remove noise. By boosting the contrast of the images from the provided MRI image collection, it is utilised to improve classification accuracy. The RGKMC segmentation procedure then incorporates these characteristics. The AFFOCNN algorithm is used to extract the key and practical characteristics throughout the feature extraction process. Finally, MCCNNs, MUNets, MFCLs, TA-cGANs, and EL algorithms combine the images in order to compare classification accuracy.The results showed that the EL method outperforms the MCCNNs, MUNets, MFCLs, and TA-cGANs algorithms in terms of classification performance, including increased accuracy, precision, recall, and lower MSEs. Future development of an optimization-based fuzzy clustering technique for managing large image datasets is possible.

References

[1]. Liu, Z., Yin, H., Chai, Y., & Yang, S. X. (2014). A novel approach for multimodal medical image fusion. *Expert systems with applications*, *41*(16), 7425-7435

[2]. Arif, Muhammad, and Guojun Wang. "Fast curvelet transform through genetic algorithm for multimodal medical image fusion." *Soft Computing* 24.3 (2020): 1815-1836.

[3]. Zhao, Wenda, Dong Wang, and Huchuan Lu. "Multi-focus image fusion with a natural enhancement via a joint multi-level deeply supervised convolutional neural network." *IEEE*

Transactions on Circuits and Systems for Video Technology 29.4 (2018): 1102-1115

[4]. Polinati, Srinivasu, et al. "The Fusion of MRI and CT Medical Images Using Variational Mode Decomposition." *Applied Sciences* 11.22 (2021): 10975.

[5]. Liu, Yu, et al. "Multi-focus image fusion with a deep convolutional neural network." *Information Fusion* 36 (2017): 191-207

[6]. Yan, Chenggang, et al. "Deep multi-view enhancement hashing for image retrieval." *IEEE Transactions on Pattern Analysis and Machine Intelligence* 43.4 (2020): 1445-1451

[7]. Tan, Wei, et al. "Multi-modal brain image fusion based on multi-level edge-preserving filtering." *Biomedical Signal Processing and Control* 64 (2021): 102280

[8]. Verma, Kesari, Bikesh Kumar Singh, and A. S. Thoke. "An enhancement in adaptive median filter for edge preservation." *Procedia Computer Science* 48 (2015): 29-36

[9]. Ibrahim, Haidi, Nicholas SiaPik Kong, and Theam Foo Ng. "Simple adaptive median filter for the removal of impulse noise from highly corrupted images." *IEEE Transactions on Consumer Electronics* 54.4 (2008): 1920-1927

[10]. Sulaiman, SitiNoraini, and NorAshidi Mat Isa. "Adaptive fuzzy-K-means clustering algorithm for image segmentation." *IEEE Transactions on Consumer Electronics* 56.4 (2010): 2661-2668

[11]. Liu, Changnian, et al. "Adaptive firefly optimization algorithm based on stochastic inertia weight." *2013 Sixth International Symposium on Computational Intelligence and Design*. Vol. 1. IEEE, 2013

[12]. Liu, Jingsen, et al. "A dynamic adaptive firefly algorithm with globally orientation." *Mathematics and Computers in Simulation* 174 (2020): 76-101

[13]. Havaei, M., Davy, A., Warde-Farley, D., Biard, A., Courville, A., Bengio, Y., ...&Larochelle, H. (2017). Brain tumor

segmentation with deep neural networks. *Medical image analysis*, *35*, 18-31.

[14]. Prakash, Om, RichaSrivastava, and AshishKhare. "Biorthogonalwavelet transform based image fusion using absolute maximum fusion rule." *2013 IEEE Conference on Information & Communication Technologies*. IEEE, 2013

[15]. Wang, Yan, et al. "3D conditional generative adversarial networks for high-quality PET image estimation at low dose." *Neuroimage* 174 (2018): 550-562

[16]. Goodfellow, I., Pouget-Abadie, J., Mirza, M., Xu, B., Warde-Farley, D., Ozair, S., ...&Bengio, Y. (2020). Generative adversarial networks. *Communications of the ACM*, *63*(11), 139-144.

[17]. Kang, Jiayin, Wu Lu, and Wenjuan Zhang. "Fusion of brain PET and MRI images using tissue-aware conditional generative adversarial network with joint loss." *IEEE Access* 8 (2020): 6368-6378

[18]. Hu, Kai, et al. "Brain tumor segmentation using multi-cascaded convolutional neural networks and conditional random field." *IEEE Access* 7 (2019): 92615-92629.